Fluorescence Quenching of 9-Aminoacridines by Purine Mononucleotides

Yukio Kubota* and Yuko Motoda

Department of Chemistry, Faculty of Science, Yamaguchi University, Yamaguchi 753, Japan *(Received: April 9, 1980; In Final Form: June 18, 1980)*

The kinetics of fluorescence quenching of 9-aminoacridine (9AA) and 9-amino-10-methylacridinium (10Me-9AA) by purine mononucleotides (adenosine 5′-monophosphate (AMP) and guanosine 5′-monophosphate (GMP)) has been studied over the temperature range of 25–46 °C in 0.1 M phosphate buffer (pH 7.0). A set of quenching parameters has been obtained on the basis of the kinetic scheme which takes into account complex formation in the ground state as well as in the excited singlet state. Both steady-state and transient fluorescence measurements have been carried out in order to determine rate constants. The rate constant for the complex formation is found to be 3.5×10^9–7×10^9 M^{-1} s^{-1}, indicating that the reaction is a diffusion-controlled one, while the rate constant for the complex dissociation is found to be much smaller than that for the complex formation. The dye–GMP complex is shown to relax nonradiatively, whereas the dye–AMP complex is accompanied by weak fluorescence and its decay kinetics obeys a double-exponential decay law. It is found that the quenching behavior for the mutagenic dye 9AA is very similar to that for the nonmutagenic dye 10Me-9AA. Thermodynamic properties for the complex formation are also discussed.

Introduction

9-Aminoacridine (9AA) is one of a number of acridine dyes that bind to DNA[1] and possess mutagenic activity.[2] Previously we have reported that the fluorescence of 9AA on binding to DNA is completely quenched by guanine–cytosine base pairs and its fluorescence decay kinetics follows a three-exponential decay law, indicating that emitting sites of 9AA consist of at least three classes.[3-5] We have also found that fluorescence behavior of 9-amino-10-methylacridinium chloride (10Me-9AA) bound to DNA is very similar to that of 9AA.[5] This result is very interesting because 10Me-9AA is nonmutagenic in contrast to 9AA.[6]

Binding interactions of dyes with DNA are considerably complex because of the content and the stereochemical arrangement of DNA bases. Recent studies on complex formation between acridine dyes and mononucleotides have shown to be useful in understanding the nature of interactions between dyes and DNA.[7-10] Therefore, it is of great interest to clarify the specific forces involved in interactions of 9AA and its derivatives with mononucleotides. Our preliminary results have shown that the fluorescence of 9AA and 10Me-9AA is markedly quenched in both dynamic and static processes by adenosine 5′-monophosphate (AMP) and guanosine 5′-monophosphate (GMP).[10]

The present investigation has been undertaken to provide additional information concerning the kinetics of fluorescence quenching for the dye–AMP and dye–GMP systems, using steady-state and transient fluorescence techniques. Individual rate constants for fluorescence quenching have been determined over the temperature range of 25–46 °C in 0.1 M phosphate buffer (pH 7.0), and the results of 9AA have been compared with those of its derivatives, 10Me-9AA and 9-methylaminoacridine (9MAA).

Experimental Section

AMP and GMP, chromatographically pure, were obtained from Sigma Chemical Co. or Seikagaku Kogyo. 9AA was the same sample as used before.[3,8] 10Me-9AA was prepared by quaternizing 9AA base with methyl iodide in methanol and by saturating a boiling concentrated aqueous solution of the dye iodide with sodium chloride.[11] 10Me-9AA was repeatedly recrystallized from hot water until no trace of unreacted 9AA was observed by the method of thin-layer chromatography. 9MAA was prepared according to the method described by Albert[12] and several times recrystallized from a methanol–ether system, and then its methanol solution was twice passed through an alumina column; no trace of impurity was detected by the method of thin-layer chromatography. 1,1,4,4-Tetraphenyl-1,3-butadiene (TPB), purchased from Tokyo Kasei, was twice recrystallized from benzene. Spectral grade cyclohexane was obtained from Wako Junyaku. Other chemicals were of reagent grade purity or better. Glass-redistilled water was used for the preparation of all aqueous solutions. Measurements were carried out at 25, 31, 38 and 46 °C in 0.1 M phosphate buffer (pH 7.0).

The absorption and fluorescence spectra were recorded with a Shimadzu UV-200S spectrophotometer and a Hitachi MPF-2A spectrophotofluorometer, respectively. For fluorescence measurements, the excitation monochromator was set at wavelengths where the change of absorbance is a minimum or at one of the isosbestic points with a 2–3-nm band-pass, and the emission was recorded with a 2-nm band-pass. Fluorescence spectra were corrected for the unequal quantum response of the detector system. Fluorescence quantum yields of dyes in the presence of mononucleotides were determined by comparing the area under the fluorescence spectrum with the corresponding area of 9AA and by taking 0.96 for the quantum yield of 9AA.[3]

Transient fluorescence decay curves were measured with an Ortec time-resolved emission spectrophotometer.[9,10] The excitation light at 375 nm was obtained with an air-filled (0.5 atm) flash lamp and an interference filter (Japan Vacuum Optics). The emission was observed by an RCA 8850 photomultiplier tube through a grating monochromator (Applied Photophysics Ltd.), the band-pass being 2–10 nm according to the fluorescence intensity of the sample. The observed fluorescence decay $i(t)$ is represented by the convolution integral:

$$i(t) = \int_0^t g(u)\, I(t-u)\, du \qquad (1)$$

where $g(t)$ is the instrument response function and $I(t)$ is the fluorescence decay which would have been obtained if the lamp flash had been infinitely short. It has been shown that the response function $g(t)$ is dependent on the

0022-3654/80/2084-2855$01.00/0

Scheme I

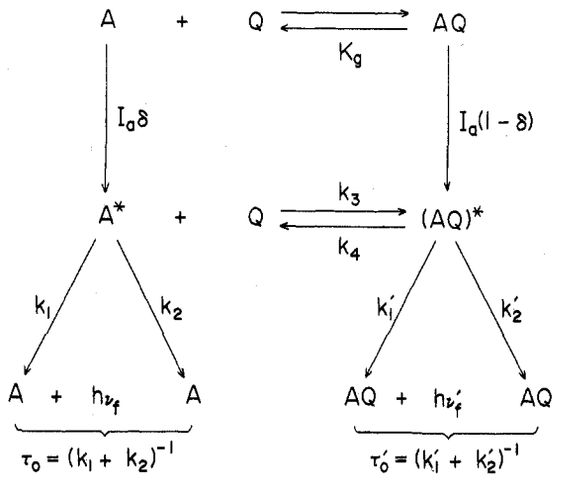

energy of photon impinging on the photocathode.[13,14] According to the method of Wahl et al.,[14] the true g(t) was determined from the fluorescence decay curve of TPB in deaerated cyclohexane which has a single-exponential decay. The lifetime of TPB was determined with excitation and emission wavelengths set at 375 and 425 nm, respectively. Under these conditions, the wavelength effect is small and g(t) could be determined by using a scattering solution.[15] The lifetime was found to be 1.72 ± 0.02 ns at 25 °C, 1.52 ± 0.02 ns at 31 °C, 1.32 ± 0.02 ns at 38 °C, and 1.18 ± 0.02 ns at 46 °C; the value at 25 °C is in good agreement with that reported by Berlman (1.76 ns).[16] Deconvolution of eq 1 was made by the methods of nonlinear least squares[17] and Laplace transformation.[15] Both methods yielded very similar results. Goodness of the fit between observed and theoretical decay curves was judged by inspection of the reduced χ^2, the weighed residuals, and the autocorrelation function of the residuals.[17] Data analysis was accomplished with a PDP 11/04 minicomputer (Digital Equipment Corp.) interfaced with an Ortec 6240B multichannel analyzer.

Kinetic Scheme for Fluorescence Quenching

Quenching data can be analyzed according to the general reaction mechanism shown in Scheme I which takes into account complex formation in the ground state as well as in the excited singlet state.[18,19] In this scheme, A and Q refer to the dye and quencher molecules, respectively, and I_a is the total light quanta absorbed by the solution. $\delta = \{1 + (\epsilon'/\epsilon)K_g[Q]\}^{-1}$ is the fraction of light absorbed by A, and $1 - \delta$ is the fraction of light absorbed by AQ, where ϵ and ϵ' are the molar extinction coefficients of A and AQ at the excitation wavelength.

For the above scheme, one has a pair of coupled ordinary differential equations:

$$d[A^*]/dt = I_a\delta + k_4[(AQ)^*] - (k_1 + k_2 + k_3[Q])[A^*] \quad (2)$$

$$d[(AQ)^*]/dt = I_a(1 - \delta) + k_3[Q][A^*] - (k_1' + k_2' + k_4)[(AQ)^*] \quad (3)$$

Under photostationary conditions, eq 2 and 3 yield[7,19]

$$\frac{\phi}{\phi_0} = \frac{\delta + k_4\tau_0' + R(1 - \delta + k_3\tau_0[Q])}{1 + k_4\tau_0' + k_3\tau_0[Q]} \quad (4)$$

where ϕ is the apparent fluorescence quantum yield of the dye in the presence of quencher and $R = \phi_0'/\phi_0$ is the ratio of the quantum yield of the complex AQ to that of free A.

For the δ-pulse excitation, integration of eq 2 and 3 with the initial conditions that at time $t = 0$ $I_a = 0$, $[A^*] = [A^*]_0$, and $[(AQ)^*] = [(AQ)^*]_0$ gives

$$[A^*] = \alpha_1 e^{-\lambda_1 t} + \alpha_2 e^{-\lambda_2 t} \quad (5)$$

$$[(AQ)^*] = \beta_1 e^{-\lambda_1 t} + \beta_2 e^{-\lambda_2 t} \quad (6)$$

where

$$\lambda_1, \lambda_2 = \tau_1^{-1}, \tau_2^{-1} = \tfrac{1}{2}[(X + Y) \mp \{(Y - X)^2 + 4k_3k_4[Q]\}^{1/2}] \quad (7)$$

$$X = k_1 + k_2 + k_3[Q] \quad (8)$$

$$Y = k_1' + k_2' + k_4 \quad (9)$$

$$\alpha_1 = \frac{1}{\lambda_2 - \lambda_1}\{[A^*]_0(\lambda_2 - X) + k_4[(AQ)^*]_0\} \quad (10)$$

$$\alpha_2 = \frac{1}{\lambda_2 - \lambda_1}\{[A^*]_0(X - \lambda_1) - k_4[(AQ)^*]_0\} \quad (11)$$

$$\beta_1 = \frac{1}{\lambda_2 - \lambda_1}\{[(AQ)^*]_0(\lambda_2 - Y) + k_3[Q][A^*]_0\} \quad (12)$$

$$\beta_2 = \frac{1}{\lambda_2 - \lambda_1}\{[(AQ)^*]_0(Y - \lambda_1) - k_3[Q][A^*]_0\} \quad (13)$$

The total fluorescence emitted by A* and (AQ)* at time t, $I_f(t)$, is given by

$$I_f(t) = k_1[A^*] + k_1'[(AQ)^*] = A_1e^{-\lambda_1 t} + A_2e^{-\lambda_2 t} \quad (14)$$

where

$$A_1 = k_1\alpha_1 + k_1'\beta_1 \quad (15)$$

$$A_2 = k_1\alpha_2 + k_1'\beta_2 \quad (16)$$

Equation 7 yields the following relationships for the λ:

$$\lambda_1 + \lambda_2 = k_1 + k_2 + k_3[Q] + k_1' + k_2' + k_4 \quad (17)$$

$$\lambda_1\lambda_2 = (k_1 + k_2)(k_1' + k_2' + k_4) + k_3(k_1' + k_2')[Q] \quad (18)$$

Once one determines λ_1, λ_2, and the unquenched lifetime τ_0, one can obtain rate constants k_3, k_4, and $k_1' + k_2'$ from plots of $\lambda_1 + \lambda_2$ and $\lambda_1\lambda_2$ against [Q]. These results are in qualitative agreement with the well-known excimer or exciplex mechanism.[20-22]

If the contribution of the complex AQ to the fluorescence emission is negligible in all circumstances, one has eq 19,

$$\phi_0' << \phi_0 \qquad k_4\tau_0' << 1 \quad (19)$$

and thus, eq 4 reduces to eq 20. In cases where eq 19

$$\phi/\phi_0 = \delta/(1 + k_3\tau_0[Q]) \quad (20)$$

holds, the decay kinetics follows a single-exponential decay law and the change in the dye fluorescence lifetime due to increasing quencher concentration is given by eq 21.

$$\tau_0/\tau = 1 + k_3\tau_0[Q] \quad (21)$$

Results and Discussion

Absorption and Fluorescence Spectra. When mononucleotides are added to a solution of 9AA or 10Me-9AA in 0.1 M phosphate buffer (pH 7.0), a specific complex is formed between the dye and the mononucleotides.[7-10] Figure 1 shows typical absorption spectra of 9AA and 10Me-9AA by varying the AMP concentration from 0 to 0.02 M. The presence of several isosbestic points in the absorption spectra indicates that both the free and complexed dye are present in the solution. From the observed absorption change, we determined, using eq 22, the

$$\frac{1}{\epsilon_{ap} - \epsilon} = \frac{1}{[Q]K_g(\epsilon' - \epsilon)} + \frac{1}{\epsilon' - \epsilon} \quad (22)$$

equilibrium constant K_g for the ground-state equilibrium (Scheme I),[9] where ϵ_{ap} is the apparent molar extinction coefficient of a dye–nucleotide solution. The K_g values thus obtained are collected in Tables I and II. As shown

TABLE I: Parameters for Fluorescence Quenching of 9AA, 10Me-9AA, and 9MAA by GMP[a]

	25 °C			31 °C		38 °C		46 °C	
	9AA	10Me-9AA	9MAA	9AA	10Me-9AA	9AA	10Me-9AA	9AA	10Me-9AA
ϕ_0	0.960	0.926	0.011	0.933	0.912	0.923	0.894	0.913	0.873
K_g,[b] M^{-1}	125	155	100	103		88		71	
K_g,[c] M^{-1}	130	150	100	110	120	95	100	73	80
K_e,[d] M^{-1}	230	260	240	192	197	160	163	124	128
$10^{-7}(k_1 + k_2)$, s^{-1}	6.33	6.17	50	6.41	6.19	6.47	6.23	6.49	6.25
$k_3^{ss}\tau_0$,[c] M^{-1}	66	73	10	75	84	86	92	93	100
$10^{-9}k_3^{ss}$,[c] M^{-1} s^{-1}	4.18	4.51	5.00	4.81	5.20	5.56	5.73	6.04	6.25
$10^{-9}k_3^{tr}$,[e] M^{-1} s^{-1}	3.48	3.70		4.17	4.27	4.85	5.05	5.65	5.88
$10^{-7}k_4$,[f] s^{-1}	1.51	1.42		2.17	2.17	3.03	3.10	4.56	4.59

[a] $\phi_0' = 0$ and $\tau_0' = 0$ for all systems. [b] From absorption data (eq 22). [c] From steady-state data (eq 20). [d] Obtained by using eq 24. [e] From transient data (eq 21). [f] From the relation $k_4 = k_3^{tr}/K_e$.

TABLE II: Parameters for Fluorescence Quenching of 9AA and 10Me-9AA by AMP

	25 °C		31 °C		38 °C		46 °C	
	9AA	10Me-9AA	9AA	10Me-9AA	9AA	10Me-9AA	9AA	10Me-9AA
ϕ_0	0.960	0.926	0.933	0.912	0.923	0.894	0.913	0.873
$R = \phi_0'/\phi_0$	0.062	0.058	0.055	0.050	0.050	0.042	0.048	0.036
K_g,[a] M^{-1}	175	200	140		110		90	
K_g,[b] M^{-1}	195	213	150	162	120	131	102	110
K_e,[c] M^{-1}	1210	500	930	390	700	310	550	250
$10^{-7}(k_1 + k_2) = 1/\tau_0$, s^{-1}	6.33	6.17	6.41	6.19	6.47	6.23	6.49	6.25
$10^{-7}k_1$,[d] s^{-1}	6.06	5.92	6.06	5.92	6.06	5.92	6.06	5.92
$10^{-6}k_2$, s^{-1}	2.7	2.5	3.5	2.7	4.1	3.1	4.3	3.3
$10^{-8}(k_1' + k_2') = 1/\tau_0'$,[e] s^{-1}	6.49	5.90	6.66	6.08	6.80	6.34	6.88	6.51
$10^{-7}k_1'$,[d] s^{-1}	4.56	4.42	4.56	4.42	4.56	4.42	4.56	4.42
$10^{-8}k_2'$, s^{-1}	6.03	5.46	6.20	5.64	6.34	5.90	6.42	6.07
$k_3^{ss}\tau_0$,[b] M^{-1}	81	81	92	92	103	101	113	110
$10^{-9}k_3^{ss}$,[b] M^{-1} s^{-1}	5.13	5.00	5.90	5.70	6.67	6.29	7.34	6.88
$10^{-9}k_3^{tr}$,[f] M^{-1} s^{-1}	3.77	3.68	4.40	4.33	5.15	5.06	5.84	5.74
$k_4\tau_0$,[b]	0.008	0.028	0.013	0.031	0.021	0.037	0.030	0.048
$10^{-6}k_4$,[b] s^{-1}	5.2	16.5	8.7	18.8	14.3	23.5	20.6	31.2
$10^{-6}k_4$,[g] s^{-1}	3.1	7.4	4.7	11.3	7.4	16.5	10.5	22.4

[a] From absorption data (eq 22). [b] From steady-state data (eq 4). [c] Obtained by using eq 24. [d] Estimated from the theory of Strickler and Berg[30] and assumed constant. [e] From slope of eq 18, using k_3^{tr}. [f] From transient data. The values obtained by using eq 17 and 23 were averaged. [g] From the relation $k_4 = k_3^{tr}/K_e$.

in Figure 1, the absorption spectra of 9AA and 10Me-9AA show red shift, slight broadening, and decrease in intensity, as a result of a specific interaction. The possibility of a stacking interaction between the acridine and purine rings has been indicated by NMR and X-ray crystallographic studies.[23] The red shift of the absorption spectra is caused by the fact that the complex formation of dyes with mononucleotides occurs more easily in the excited state than in the ground state. This will be discussed later.

The progressive change of the fluorescence spectra of 9AA and 10Me-9AA with increasing AMP concentration is illustrated in Figure 2, A and B. This change shows that the fluorescence spectrum can be assigned to the superposition of emissions of both the free and complexed dye. At a sufficiently high concentration of AMP (above 0.05 M), the complexed dye predominantly contributes to the total fluorescence. As in the absorption spectrum, red shift and broadening of the fluorescence spectrum are also observed as a result of complex formation. The fluorescence spectrum displays a good image of the absorption spectrum obtained under the same conditions. The change in shape of the fluorescence spectrum is accompanied by a strong fluorescence quenching.

On the other hand, the presence of GMP also caused a strong quenching of the dye fluorescence. However, the fluorescence and fluorescence-excitation spectra of the dye in the presence of GMP were identical with the corresponding spectra of the free dye. This implies that (AQ)* is nonfluorescent in the dye–GMP system.[8]

Transient Kinetics. As expected from the proposed kinetic scheme, we experimentally observed a single-exponential fluorescence decay for the dye–GMP system and

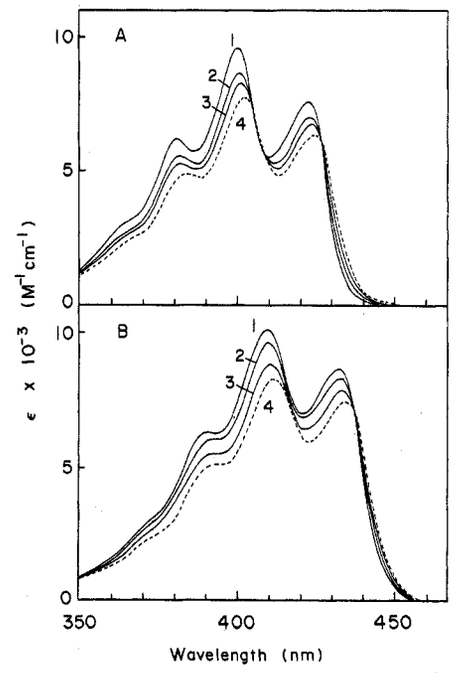

Figure 1. Absorption spectra of (A) 9AA and (B) 10Me-9AA in the presence of AMP in 0.1 M phosphate buffer (pH 7.0) at 25 °C. (A) 9AA: 6.0×10^{-5} M. AMP: (1) 0 M (free); (2) 3.9×10^{-3} M; (3) 7.1×10^{-3} M; (4) 2.0×10^{-2} M. (B) 10Me-9AA: 5.0×10^{-5} M. AMP: (1) 0 M (free); (2) 2.0×10^{-3} M; (3) 8.6×10^{-3} M; (4) 2.0×10^{-2} M.

a double-exponential fluorescence decay for the dye–AMP system. Typical decay curves obtained with the 9AA–

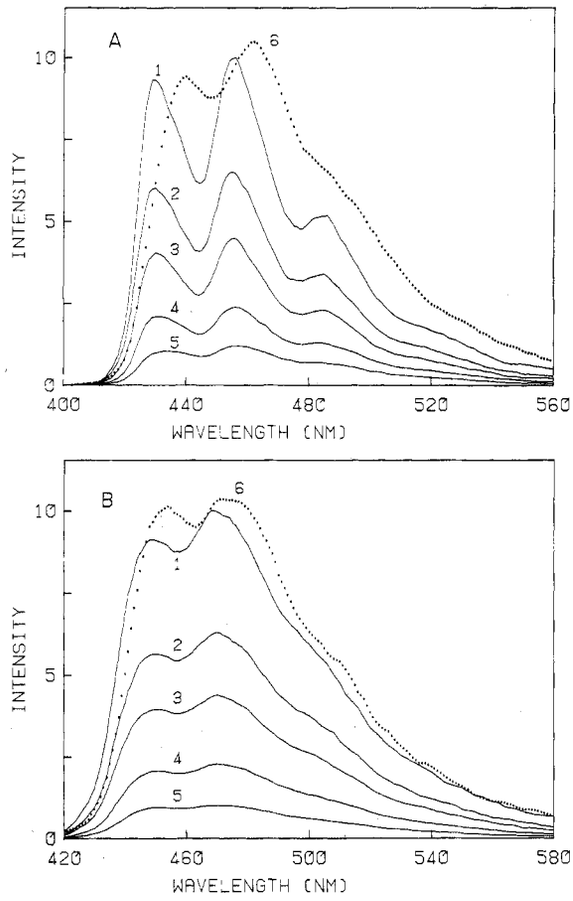

Figure 2. Change in the fluorescence spectra of (A) 9AA and (B) 10Me-9AA with increasing AMP concentration at 25 °C. The excitation wavelengths were 405 and 415 nm, respectively, for 9AA and 10Me-9AA. The spectra were corrected for distortions caused by scattering. The dye concentration was 1.2×10^{-5} M. AMP: (1) 0 M (free); (2) 2.0×10^{-3} M; (3) 4.0×10^{-3} M; (4) 1.0×10^{-2} M; (5) 2.0×10^{-2} M; (6) 5.0×10^{-2} M (×15).

GMP and 9AA–AMP systems are shown in Figures 3 and 4. In all cases, the χ^2 values (χ^2 = 1.0–2.0), the weighed residuals, and the autocorrelation function of the residuals indicated that the decay data obtained with the dye–GMP system is consistent with a single-exponential decay law, whereas that obtained with the dye–AMP system is compatible with a double-exponential decay law. At a low AMP concentration (below 4×10^{-3}–6×10^{-3} M) in which the contribution of the complex AQ to the fluorescence emission is small, however, the decay kinetics followed a single-exponential decay law rather than a double-exponential one. There was no variation in the lifetimes with emission wavelength. Several determinations of the lifetime were made, and the average value was used for the following analyses.

The change in the dye fluorescence lifetime due to increasing GMP concentration over the temperature range of 25–46 °C is shown by the plots of τ_0/τ vs. [Q] in Figure 5. The values of k_3 can be calculated from the slopes of these plots by using eq 21 and are given in Table I.

Figure 6 displays plots of the decay parameters associated with $A_1e^{-\lambda_1 t} + A_2e^{-\lambda_2 t}$ for 9AA and 10Me-9AA quenched by AMP. A nearly linear increase of λ_1 and a slight decrease of λ_2 with increasing AMP concentration can be seen. A plot of $\lambda_1 + \lambda_2$ vs. [Q] was approximately linear with the scatter. This plot should have a slope of k_3 and an intercept of $k_1 + k_2 + k_1' + k_2' + k_4$ according to eq 17. The intercept of λ_2 as well as the known $k_1 + k_2$ can be used to obtain a point for the intercept of the plot $\lambda_1 + \lambda_2$; this procedure is helpful in obtaining the best

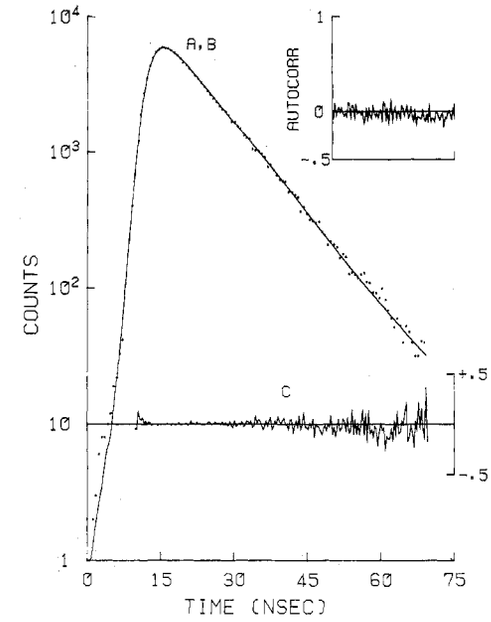

Figure 3. Observed decay curves and the results of an analysis for a single exponential for the 9AA–GMP system at 38 °C. The excitation and emission wavelengths were 375 and 455 nm, respectively. 9AA: 1.2×10^{-5} M. GMP: 1.0×10^{-2} M. A: Observed decay curve. B: Best theoretical decay curve (smooth curve) based on the lifetime τ = 9.01 ns (χ^2 = 1.71). C: Weighed residuals. The inset is the autocorrelation function of the residuals.

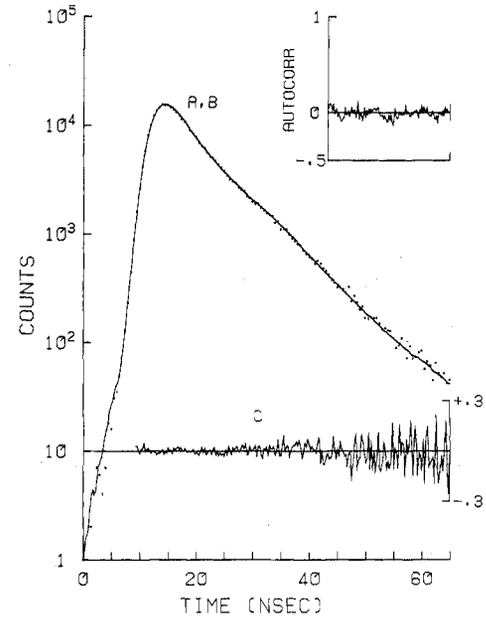

Figure 4. Double-exponential analysis of the decay of the 9AA–AMP system at 25 °C. The excitation and emission wavelengths were 375 and 460 nm, respectively. 9AA: 1.2×10^{-5} M. AMP: 2.0×10^{-2} M. The best theoretical decay curve is based on the following decay parameters: τ_1 = 7.61 ns, τ_2 = 1.53 ns, A_1 = 0.123, and A_2 = 0.257 (χ^2 = 1.48).

estimate for the slope and thus k_3. An alternative method of obtaining k_3 is to use the initial slope of a plot of λ_1 vs. [Q]:

$$\lim_{[Q]\to 0} \frac{\Delta\lambda_1}{\Delta[Q]} = k_3 \qquad (23)$$

The average values for k_3 determined by both methods are given in Table II.

The slope of the plot of $\lambda_1\lambda_2$ vs. [Q] shown in Figure 7 can be used, along with the known k_3, to obtain the value of $k_1' + k_2'$ (Table II). However, k_4 could not be estimated

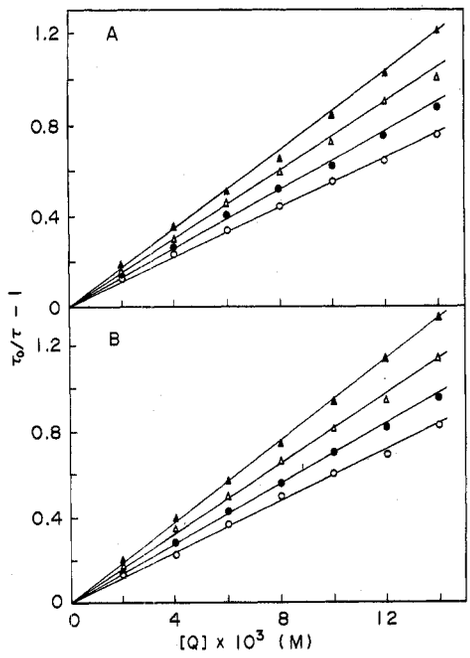

Figure 5. Change in the fluorescence lifetimes of (A) 9AA and (B) 10Me-9AA with increasing GMP concentration: (O) 25 °C; (●) 31 °C; (Δ) 38 °C; (▲) 46 °C.

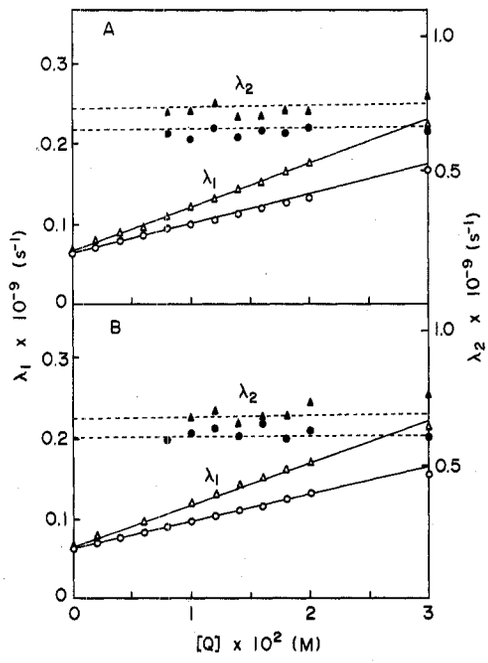

Figure 6. Plots of the decay parameters associated with $A_1e^{-\lambda_1 t} + A_2e^{-\lambda_2 t}$ for (A) 9AA and (B) 10Me-9AA quenched by AMP. Solid and broken lines show the calculated data using eq 7. (O, ●) 25 °C; (Δ, ▲) 46 °C.

directly from the plots shown in Figures 6 and 7, since k_4 was very small compared to the sum $(k_1' + k_2')$ (Table II).

Steady-State Kinetics. The change in the fluorescence yields of 9AA and 10Me-9AA, in the absence (ϕ_0) and the presence (ϕ) of quencher, with increasing quencher concentration is shown in Figure 8, A and B. Evidently the experimental data deviate greatly from linearity, which is indicative of more than one quenching processes (Scheme I). The ratios of the quantum yield of the complex AQ to that of the free A, $R = \phi_0'/\phi_0$, were found to be zero and nonzero for the dye–GMP and dye–AMP systems, respectively, by extrapolating the apparent quantum yield ϕ to infinite quencher concentration. The R values for the dye–AMP system are given in Table II.

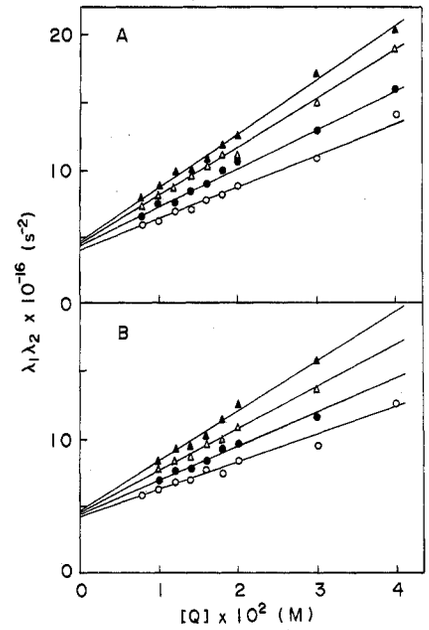

Figure 7. $\lambda_1\lambda_2$ vs. [Q] for (A) 9AA–AMP and (B) 10Me systems: (O) 25 °C; (●) 31 °C; (Δ) 38 °C; (▲) 46 °C.

To obtain steady-state quenching parameters, we carried out nonlinear regression analysis[24] by employing eq 20 and 4 for the dye–GMP and dye–AMP systems, respectively, in which δ, $k_3\tau_0$, and $k_4\tau_0'$ were taken as the unknown parameters and R was taken as the known parameter. $\tau_0 = (k_1 + k_2)^{-1}$ and $\tau_0' = (k_1' + k_2')^{-1}$ determined from transient experiments were used to calculate rate constants k_3 and k_4. A set of parameters thus obtained are summarized in Tables I and II. K_g is a little higher than the value obtained from the absorption data, but the agreement between both values seems to be satisfactory within limits of experimental error (±4–8% standard deviations). Using steady-state quenching parameters given in Tables I and II, we computed eq 20 and 4 for $0 < [Q] < 0.02$ M and compared them with the experimental data (Figure 8). The fit between the computed and experimental data appears to be gratifying.

Equilibrium Constant for the Excited-State Equilibrium. The equilibrium constant K_e for the excited-state equilibrium can be estimated from K_g and from the spectral shift due to the complex formation, using the approximate equation:[18,25]

$$\log K_e = \log K_g + (0.625/T)\Delta\nu \qquad (24)$$

where $\Delta\nu$ is the 0–0 band shift in cm^{-1} of the free and complexed dye for the $S_0 \rightarrow S_1$ transition. The $\Delta\nu$ values for the dye–GMP system were estimated from the absorption spectral shifts because the fluorescence spectrum of the complexed dye was not detectable, whereas those for the dye–AMP system were estimated from both the absorption and fluorescence spectra. In all systems, the $\Delta\nu$ values were almost constant over the temperature range investigated.

The K_e values obtained are given in Tables I and II. In all systems, K_e is found to be much larger than K_g. The rate constant for complex dissociation (k_4) can be estimated by using the relation $k_4 = k_3/K_e$. The resultant values for k_4 in Tables I and II are obtained by using the forward rate constant determined from transient experiments (k_3^{tr}).

Discussion of Rate Constants. All quenching parameters obtained from both transient and steady-state experiments are summarized in Tables I and II. The results presented in this paper are in qualitative agreement with

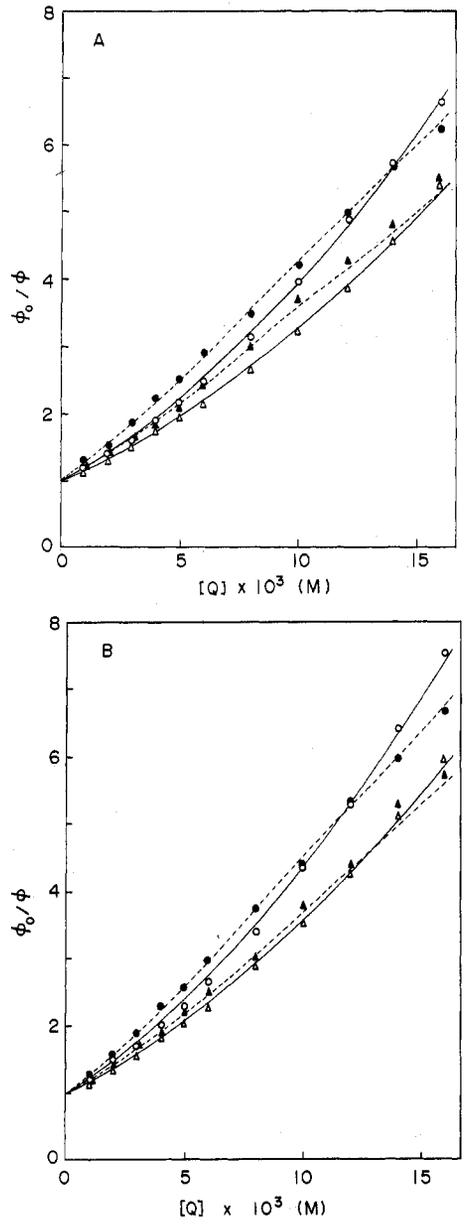

Figure 8. Best fit between experimental and calculated data for the change in the fluorescence yields of (A) 9AA and (B) 10Me-9AA with increasing quencher concentration. Solid and broken lines are the calculated data using eq 20 and 4, respectively: (○) GMP (25 °C); (△) GMP (46 °C); (●) AMP (25 °C); (▲) AMP (46 °C).

those obtained by using 0.005 M phosphate buffer as solvent.[10] The magnitudes reported for the rate constant k_3 are as expected for a diffusion-controlled forward reaction.[26] The decrease of k_3 with decreasing temperature is consistent with a concomitant decrease in the diffusion coefficients of A* and Q with temperature. For both quenchers AMP and GMP, the forward rate constant obtained from steady-state experiments (k_3^{ss}) is found to be slightly larger than that obtained from transient experiments (k_3^{tr}). This discrepancy may be due to transient effects associated with diffusion.[22,27,28] When diffusion effects are taken into account, $k_3^{ss}\tau_0$ can be expressed by $k_3^{tr}\tau_0[1 + R'/(\tau_0 D)^{1/2}]$,[22,27,28] where R' is the effective quenching radius for the encounter pair and D is the sum of the diffusion coefficients for A and Q. From the experimental discrepancy between k_3^{ss} and k_3^{tr} (Tables I and II) and using 6×10^{-6} and 4×10^{-6} cm^2 s^{-1}, respectively, for the diffusion coefficients of A and Q at 25 °C,[25,29] we obtain $R' \simeq 8$ Å for GMP and $R' \simeq 14$ Å for AMP as the quencher.

TABLE III: Thermodynamic Properties and Activation Energies[a]

	9AA-GMP	9AA-AMP	10Me-9AA-GMP	10Me-9AA-AMP
ΔG_g°, kcal mol^{-1}	−2.88	−3.12	−2.97	−3.18
ΔH_g°, kcal mol^{-1}	−4.87	−5.66	−5.17	−5.76
ΔS_g°, eu	−6.67	−8.52	−7.38	−8.65
ΔG_e°, kcal mol^{-1}	−3.22	−4.21	−3.29	−3.68
ΔH_e°, kcal mol^{-1}	−5.76	−7.35	−6.26	−6.86
ΔS_e°, eu	−8.52	−10.55	−9.96	−10.67
$\Delta E_2^\ddagger$, kcal mol^{-1}	4.57	4.22	4.57	4.17
$\Delta E_4^\ddagger$, kcal mol^{-1}	10.33	11.52	10.83	11.13
$\Delta E_2^\ddagger$, kcal mol^{-1}		4.2		3.3
$\Delta E_{2'}^\ddagger$, kcal mol^{-1}		0.9		1.1

[a] The subscripts g and e, respectively, refer to the ground-state and excited-state complex formation. The values of ΔG° and ΔS° are those obtained at 25 °C.

It is of interest to compare k_3 and the backward rate constant k_4. Over the temperature range of 25–46 °C, k_4 is found to be much smaller than k_3, in harmony with the finding $K_e >> K_g$. The k_4 values determined from steady-state data are approximately twice those calculated from the relation $k_4 = k_3^{tr}/K_e$ (Table II). If we adopt k_3^{ss} instead of k_3^{tr} in the relation $k_4 = k_3/K_e$, however, the resultant values for k_4 are in reasonable agreement with the values obtained from steady-state data (eq 4) within the experimental error. The above discrepancy may be ascribed to overestimation of k_3^{ss} and thus k_4 in steady-state measurements which results from transient effects.

Using rate constants obtained from transient experiments, we computed eq 7 for $0 < [Q] < 0.03$ M and compared it with the experimental data (Figure 6). It can be seen that the fit between the computed and experimental data is quite satisfactory.

In order to separate the sum $(k_1 + k_2)$ or $(k_1' + k_2')$ into individual rate constants, the radiative rate constants for the free and complexed dye (k_1 and k_1') were evaluated according to the theory of Strickler and Berg[30] from the spectral data. The resultant values are given in Table II. On the other hand, the radiative rate constants can be also estimated, using the relation $k_1 = \phi_0/\tau_0$ or $k_1' = \phi_0'/\tau_0'$ from the observed quantum yield and lifetime. The k_1 values thus obtained are in good agreement with the theoretical values and are nearly constant over the temperature range in question, while the k_1' values are a little smaller than the theoretical ones. This may be due, in part, to the errors involved in calculations for the sum $(k_1' + k_2')$ and ϕ_0'. Since both the absorption and fluorescence spectra are almost unchanged over the temperature range of 25–46 °C, we assume that k_1 and k_1' are constant irrespective of the temperature. Using the theoretical values for k_1 and k_1', we evaluated the nonradiative rate constants k_2 and k_2' and the results are also given in Table II.

Thermodynamic Properties and Activation Energies. From van't Hoff plots of the logarithm of the equilibrium constants (K) vs. $1/T$ and using the relations $\Delta G^\circ = -RT \ln K$ and $\Delta H^\circ = \Delta G^\circ - T\Delta S^\circ = -R\, d \ln K/d(1/T)$, one can obtain thermodynamic quantities for complex formation in both the ground and excited states (Table III). The results of the 9AA–GMP system are consistent with those obtained in 0.005 M phosphate buffer.[8] The entropy change ΔS° was found to be constant regardless of the temperature, and negative values for ΔS° suggest a tight and rigid geometry of the complex in both the ground and excited states. The magnitudes of ΔH_e°[31] and ΔS_e° are somewhat larger than those of ΔH_g° and ΔS_g°. This means that the excitation of the dye may result in the increased stability of the complex.

Arrhenius plots for k_3^{tr} give a straight line with the slope of the activation energy $\Delta E_3^{\ddagger} = 4.17$–$4.57$ kcal mol^{-1} (Table III). These values are in good agreement with the value (4.3 kcal mol^{-1}) expected for the diffusion-controlled reaction in water.[26] Using ΔH_e° and $\Delta E_3^{\ddagger}$, one can estimate $\Delta E_4^{\ddagger}$ since $K_e = k_3/k_4$ and $\Delta H_e^\circ = \Delta E_3^{\ddagger} - \Delta E_4^{\ddagger}$. The resultant values are also shown in Table III. The fact that $\Delta E_4^{\ddagger}$ is much larger than $\Delta E_3^{\ddagger}$ is consistent with the finding $k_4 << k_3$.

Arrhenius plots also permit a rough estimation for the activation energies associated with k_2 and k_2' (Table III). The error introduced in calculating k_2 and k_2' may not affect, in any significant way, subsequent calculation of $\Delta E_2^{\ddagger}$ and $\Delta E_{2'}^{\ddagger}$, which involves logarithms of rate constants. It should be noted that the magnitude of $\Delta E_2^{\ddagger}$ is very close to the energy difference between vibrational levels (3.8 kcal mol^{-1} for 9AA and 2.9 kcal mol^{-1} for 10Me-9AA). Internal conversion may be important for relaxation of the fluorescence state of the free dye. On the other hand, the finding $\Delta E_{2'}^{\ddagger} << \Delta E_2^{\ddagger}$ implies that there exist different deactivation paths for the complexed dye.

Fluorescence Behavior of 9MAA. The results presented here clearly indicate that the quenching behavior for the nonmutagenic dye 10Me-9AA is very similar to that for the mutagenic dye 9AA. It is now interesting to compare the fluorescence behavior of 9MAA with that of 9AA and 10Me-9AA. It was found that the fluorescence of 9MAA was quenched by GMP, but enhanced by AMP. As shown in Table I, the quenching behavior of the 9MAA–GMP system is similar to that of the 9AA–GMP and 10Me-9AA–GMP systems. In view of the results for 9AA, 10Me-9AA, and 9MAA, the 9-amino substituent of the acridine ring may play an important role in the quenching behavior.

Possible Explanations for Fluorescence Quenching. The magnitudes of ΔH° and ΔS° are as expected for charge transfer and for hydrogen bonding interactions. In view of the good electron-acceptor ability of acridines[32] and the low ionization potential of guanine as compared with other DNA bases,[33] charge transfer between guanine and acridines would be possible for one of nonradiative processes. In practice GMP quenches the fluorescence of proflavin,[7] acriflavin,[34] quinacrine,[34] and 10-methylacridinium[9] in addition to acridines examined in this study. It is somewhat surprising that AMP still acts as the quencher for 9AA and 10Me-9AA although the electron-donor ability of adenine is poorer than that of guanine.[33] Perhaps 9AA and 10Me-9AA may possess better electron-acceptor ability than proflavin because 9AA shows a higher reduction potential than proflavin.[35] On the other hand, the small value of $\Delta E_2^{\ddagger}$ would suggest another possibility, intersystem crossing in (AQ)*, for nonradiative relaxation of (AQ)*. At present, however, there is no convincing evidence for the quenching mechanism. Indeed the study of transient intermediates by laser photolysis may answer the problem.

Finally, the above results for 9AA and 10Me-9AA and the results for 10-methylacridinium showing no mutagenicity[9] suggest that there might not be a direct relationship between the quenching behavior and the mutagenicity.[36] It is expected that even a small change in the dye structure may exert a large effect on binding interactions of the dye with DNA.[1] Perhaps the geometry of the dye bound to DNA may be rather important in the biological activity of the dye.

Acknowledgment. This work was supported by a Grant-in-Aid for Scientific Research from the Ministry of Education of Japan. We thank Dr. Ludwig Brand for providing listings of computer programs for the method of nonlinear least squares.

References and Notes

(1) A. R. Peacocke, "Heterocyclic Compounds: Acridines", Vol. 9, R. M. Acheson, Ed., Interscience, New York, 1973, p 723.
(2) A. Orgel and S. Brenner, *J. Mol. Biol.*, **3**, 762 (1961).
(3) Y. Kubota, K. Hirano, and Y. Motoda, *Chem. Lett.*, 123 (1978).
(4) Y. Kubota, Y. Motoda, and Y. Fujisaki, *Chem. Lett.*, 237 (1979).
(5) Y. Kubota and Y. Motoda, *Biochemistry*, in press.
(6) L. S. Lerman, *J. Cell. Comp. Physiol.*, **64**, Supplement 1, 1 (1964).
(7) M. G. Badea and S. Georghiou, *Photochem. Photobiol.*, **24**, 417 (1976).
(8) Y. Kubota, *Chem. Lett.*, 311 (1977).
(9) Y. Kubota, Y. Motoda, Y. Shigemune, and Y. Fujisaki, *Photochem. Photobiol.*, **29**, 1099 (1979).
(10) Y. Kubota and Y. Motoda, *Chem. Lett.*, 1375 (1979).
(11) A. Albert and B. Ritchie, *J. Chem. Soc.*, 458 (1943).
(12) A. Albert, "The Acridines", 2nd ed., Arnold, London, 1965, p 307.
(13) C. Lewis, W. R. Ware, L. J. Doemeny, and T. L. Nemzek, *Rev. Sci. Instrum.*, **44**, 107 (1973).
(14) P. Wahl, J. C. Auchet, and B. Donzel, *Rev. Sci. Instrum.*, **45**, 28 (1974).
(15) A. Gafni, R. L. Modlin, and L. Brand, *Biophys. J.*, **15**, 263 (1975).
(16) I. B. Berlman, "Handbook of Fluorescence Spectra of Aromatic Molecules", 2nd ed., Academic Press, New York, 1971, p 321.
(17) A. Grinvald and I. Z. Steinberg, *Anal. Biochem.*, **59**, 583 (1974).
(18) A. Weller, *Prog. React. Kinet.*, **1**, 189 (1961).
(19) W. M. Vaughan and G. Weber, *Biochemistry*, **9**, 464 (1970).
(20) J. B. Birks, "Photophysics of Aromatic Molecules", Wiley-Interscience, New York, 1970, Chapter 7; "Organic Molecular Photophysics", Vol. 2, J. B. Birks, Ed., Wiley-Interscience, New York, 1973, Chapter 9.
(21) W. R. Ware, D. Watt, and J. D. Homes, *J. Am. Chem. Soc.*, **96**, 7853 (1974).
(22) M. H. Hui and W. R. Ware, *J. Am. Chem. Soc.*, **98**, 4718 (1976).
(23) F. E. Hruska and S. S. Danyluk, *Biochim. Biophys. Acta*, **161**, 250 (1968); T. D. Sakore, S. C. Jain, C. C. Tsai, and H. M. Sobell, *Proc. Natl. Acad. Sci. U.S.A.*, **74**, 188 (1977); J. Rueben, B. M. Baker, and N. R. Kallenback, *Biochemistry*, **17**, 2915 (1978).
(24) P. R. Bevington, "Data Reduction and Error Analysis for the Physical Sciences", McGraw-Hill, New York, 1969, Chapter 11.
(25) A. Weller, *Z. Elektrochem.*, **61**, 956 (1957).
(26) C. A. Parker, "Photoluminescence of Solutions", Elsevier, Amsterdam, 1968, p 74.
(27) W. R. Ware and J. S. Novros, *J. Phys. Chem.*, **70**, 3246 (1966).
(28) M. H. Hui and W. R. Ware, *J. Am. Chem. Soc.*, **98**, 4712 (1976).
(29) G. Schramm, W. Albrecht, and K. Munk, *Z. Naturforsch. B* **7**, 10 (1952).
(30) S. J. Strickler and R. A. Berg, *J. Chem. Phys.*, **37**, 814 (1962).
(31) The subscripts g and e, respectively, refer to the ground-state and excited-state complex formation.
(32) B. Pullman, *C. R. Hebd. Seances Acad. Sci.*, **255**, 3255 (1962); J. A. Singer and W. P. Purcell, *J. Med. Chem.*, **10**, 754 (1967).
(33) V. A. Bloomfield, D. M. Crothers, and I. Tinoco, Jr., "Physical Chemistry of Nucleic Acids", Harper and Row, New York, 1974, p 53, and references cited therein.
(34) Y. Kubota and Y. Motoda, unpublished results.
(35) B. Breyer, G. S. Buchanan, and H. Duewell, *J. Chem. Soc.*, 360 (1944).
(36) J. P. Schreiber and M. P. Daune, *J. Mol. Biol.*, **83**, 487 (1974).